ACTA ASTRONOMICA
Vol. **58** (2008) pp. 89–102

The Optical Gravitational Lensing Experiment. OGLE-III Photometric Maps of the Large Magellanic Cloud*

A. Udalski[1], I. Soszyński[1], M.K. Szymański[1], M. Kubiak[1], G. Pietrzyński[1,2], Ł. Wyrzykowski[3,1], O. Szewczyk[2,1], K. Ulaczyk[1] and R. Poleski[1]

[1] Warsaw University Observatory, Al. Ujazdowskie 4, 00-478 Warszawa, Poland
e-mail: (udalski,soszynsk,msz,mk,pietrzyn,wyrzykow,szewczyk,kulaczyk,rpoleski)
@astrouw.edu.pl
[2] Universidad de Concepción, Departamento de Fisica, Casilla 160–C, Concepción, Chile
[3] Institute of Astronomy, University of Cambridge, Madingley Road, Cambridge
CB3 0HA, UK

Received June 27, 2008

ABSTRACT

We present the OGLE-III Photometric Maps of the Large Magellanic Cloud. They cover about 40 square degrees of the LMC and contain mean, calibrated *VI* photometry and astrometry of about 35 million stars observed during seven observing seasons of the third phase of the Optical Gravitational Lensing Experiment – OGLE-III.

We discuss the quality of data and present color–magnitude diagrams of selected fields. The OGLE-III Photometric Maps of the LMC are available to the astronomical community from the OGLE Internet archive.

Key words: *Magellanic Clouds – Surveys – Catalogs – Techniques: photometric*

1. Introduction

One of the important results of the second phase of the Optical Gravitational Lensing Experiment was publication of the OGLE Photometric Maps of Dense Stellar Regions (Udalski *et al.* 1998, 2000, 2002) containing precisely calibrated *BVI* photometry and astrometry of the SMC, LMC and Galactic bulge fields observed during OGLE-II. Because these regions of the sky are extremely interesting from the astrophysical point of view, OGLE maps have been widely used by astronomers worldwide for many astrophysical applications.

OGLE-III phase of the OGLE project, started on June 12, 2001 and still in operation, was a significant extension of the OGLE survey. Much larger observing capabilities made it possible to cover practically entire area of the LMC and

*Based on observations obtained with the 1.3 m Warsaw telescope at the Las Campanas Observatory of the Carnegie Institution of Washington.

SMC and large fraction of the Galactic bulge. After seven years of continuous observations the huge collection of OGLE images was re-reduced to obtain the final precise photometry, calibrated to the standard system (Udalski *et al.* 2008). Thus it became possible to extend the OGLE-II maps to new regions, not observed by OGLE before.

In this paper we present the OGLE-III photometric maps of the Large Magellanic Cloud. They are available to the astronomical community from the OGLE Internet archive.

2. Observations

OGLE-III images of the LMC used for construction of the OGLE-III Photometric Maps of this galaxy were collected between July 2001 and March 2008 and cover seven observing seasons of the LMC. Observations were carried out at Las Campanas Observatory, operated by the Carnegie Institution of Washington, with 1.3 m Warsaw telescope equipped with the eight chip mosaic camera (Udalski 2003). One full mosaic image covers approximately $35' \times 35'$ on the sky with the scale of $0\farcs26$/pixel.

As the main goal of the OGLE survey is the search for variability of observed objects, the majority of observations were obtained through the single, namely I-band filter. Although this filter well approximates the standard one for $V-I<3$ mag colors, one has to be aware that for very red objects some deviation may be present. Several hundred I-band images were collected for each of the observed fields. From time to time the LMC fields were also observed in the V-band – typically about 40–50 times in the considered period. The exposure time was set to 180 and 240 seconds in the I and V-band, respectively.

Because the majority of observed fields have high stellar density, observations were conducted only in good seeing and transparency conditions. When the seeing exceeded $1\farcs8$ observations were stopped. The median seeing of the V and I-band OGLE-III LMC datasets is equal to $1\farcs2$.

Table 1 lists all LMC fields observed during OGLE-III phase. It also provides equatorial coordinates of their centers and number of stars detected in the I-band. The total observed area reaches 40 square degrees. Fig. 1 presents a combined image of the LMC taken by the ASAS survey program (Pojmański, 1997) with contours of the OGLE-II and OGLE-III fields.

3. Data Reductions

Initial pre-reductions of the collected images – de-biasing, flatfielding – are done at the telescope, immediately after the last pixel of the image is written to the main data acquisition computer (Udalski 2003). Although the first, provisional ph-

T a b l e 1

OGLE-III Fields in the LMC

Field	RA (2000)	DEC (2000)	$N_{\rm Stars}$
LMC100	$5^{\rm h}19^{\rm m}02.^{\rm s}2$	$-69^\circ15'07''$	1075711
LMC101	$5^{\rm h}19^{\rm m}03.^{\rm s}1$	$-68^\circ39'19''$	548707
LMC102	$5^{\rm h}19^{\rm m}03.^{\rm s}4$	$-68^\circ03'48''$	266963
LMC103	$5^{\rm h}19^{\rm m}02.^{\rm s}9$	$-69^\circ50'26''$	833034
LMC104	$5^{\rm h}19^{\rm m}02.^{\rm s}4$	$-70^\circ26'03''$	472959
LMC105	$5^{\rm h}19^{\rm m}01.^{\rm s}6$	$-71^\circ01'31''$	353469
LMC106	$5^{\rm h}19^{\rm m}01.^{\rm s}0$	$-71^\circ36'57''$	236384
LMC107	$5^{\rm h}13^{\rm m}01.^{\rm s}5$	$-66^\circ52'57''$	226287
LMC108	$5^{\rm h}13^{\rm m}01.^{\rm s}9$	$-67^\circ28'40''$	257801
LMC109	$5^{\rm h}12^{\rm m}53.^{\rm s}3$	$-68^\circ04'06''$	294145
LMC110	$5^{\rm h}12^{\rm m}43.^{\rm s}6$	$-68^\circ39'42''$	529605
LMC111	$5^{\rm h}12^{\rm m}32.^{\rm s}7$	$-69^\circ15'02''$	696121
LMC112	$5^{\rm h}12^{\rm m}21.^{\rm s}5$	$-69^\circ50'21''$	752907
LMC113	$5^{\rm h}12^{\rm m}10.^{\rm s}9$	$-70^\circ25'48''$	561679
LMC114	$5^{\rm h}11^{\rm m}58.^{\rm s}9$	$-71^\circ01'22''$	221912
LMC115	$5^{\rm h}07^{\rm m}09.^{\rm s}7$	$-66^\circ52'59''$	234177
LMC116	$5^{\rm h}07^{\rm m}00.^{\rm s}9$	$-67^\circ28'29''$	205536
LMC117	$5^{\rm h}06^{\rm m}55.^{\rm s}3$	$-68^\circ03'58''$	527346
LMC118	$5^{\rm h}06^{\rm m}25.^{\rm s}4$	$-68^\circ39'25''$	694697
LMC119	$5^{\rm h}06^{\rm m}02.^{\rm s}5$	$-69^\circ15'02''$	817851
LMC120	$5^{\rm h}05^{\rm m}39.^{\rm s}8$	$-69^\circ50'28''$	617701
LMC121	$5^{\rm h}05^{\rm m}14.^{\rm s}4$	$-70^\circ25'59''$	442352
LMC122	$5^{\rm h}04^{\rm m}52.^{\rm s}9$	$-71^\circ01'25''$	288282
LMC123	$5^{\rm h}01^{\rm m}18.^{\rm s}0$	$-66^\circ53'00''$	242827
LMC124	$5^{\rm h}01^{\rm m}00.^{\rm s}3$	$-67^\circ28'27''$	290411
LMC125	$5^{\rm h}00^{\rm m}36.^{\rm s}1$	$-68^\circ03'54''$	357288
LMC126	$5^{\rm h}00^{\rm m}02.^{\rm s}4$	$-68^\circ39'31''$	530735
LMC127	$4^{\rm h}59^{\rm m}33.^{\rm s}6$	$-69^\circ14'54''$	547901
LMC128	$4^{\rm h}59^{\rm m}03.^{\rm s}6$	$-69^\circ50'24''$	406243
LMC129	$4^{\rm h}58^{\rm m}24.^{\rm s}6$	$-70^\circ26'07''$	304616
LMC130	$4^{\rm h}57^{\rm m}50.^{\rm s}8$	$-71^\circ01'20''$	231039
LMC131	$4^{\rm h}55^{\rm m}28.^{\rm s}6$	$-66^\circ52'46''$	248421
LMC132	$4^{\rm h}55^{\rm m}00.^{\rm s}6$	$-67^\circ28'36''$	217827
LMC133	$4^{\rm h}54^{\rm m}29.^{\rm s}2$	$-68^\circ03'47''$	346558
LMC134	$4^{\rm h}53^{\rm m}49.^{\rm s}2$	$-68^\circ39'18''$	304271
LMC135	$4^{\rm h}53^{\rm m}05.^{\rm s}2$	$-69^\circ14'51''$	284846
LMC136	$4^{\rm h}52^{\rm m}23.^{\rm s}7$	$-69^\circ50'25''$	244490
LMC137	$4^{\rm h}51^{\rm m}30.^{\rm s}2$	$-70^\circ26'01''$	200058
LMC138	$4^{\rm h}49^{\rm m}34.^{\rm s}7$	$-66^\circ53'07''$	117664
LMC139	$4^{\rm h}49^{\rm m}05.^{\rm s}2$	$-67^\circ28'30''$	128858
LMC140	$4^{\rm h}48^{\rm m}18.^{\rm s}2$	$-68^\circ04'05''$	188164
LMC141	$4^{\rm h}47^{\rm m}26.^{\rm s}7$	$-68^\circ39'36''$	191197
LMC142	$4^{\rm h}46^{\rm m}31.^{\rm s}9$	$-69^\circ15'08''$	225807
LMC143	$4^{\rm h}45^{\rm m}43.^{\rm s}1$	$-69^\circ50'19''$	155672
LMC144	$4^{\rm h}44^{\rm m}40.^{\rm s}2$	$-70^\circ26'01''$	116363
LMC145	$4^{\rm h}43^{\rm m}47.^{\rm s}5$	$-66^\circ52'43''$	64628
LMC146	$4^{\rm h}43^{\rm m}03.^{\rm s}0$	$-67^\circ28'17''$	86656
LMC147	$4^{\rm h}42^{\rm m}07.^{\rm s}8$	$-68^\circ03'55''$	103604
LMC148	$4^{\rm h}41^{\rm m}06.^{\rm s}8$	$-68^\circ39'27''$	110885
LMC149	$4^{\rm h}40^{\rm m}05.^{\rm s}1$	$-69^\circ14'57''$	115117
LMC150	$4^{\rm h}39^{\rm m}05.^{\rm s}3$	$-69^\circ50'16''$	96039
LMC151	$4^{\rm h}37^{\rm m}51.^{\rm s}6$	$-70^\circ25'45''$	89935
LMC152	$4^{\rm h}37^{\rm m}54.^{\rm s}1$	$-66^\circ52'52''$	46107
LMC153	$4^{\rm h}37^{\rm m}01.^{\rm s}7$	$-67^\circ28'30''$	56016
LMC154	$4^{\rm h}35^{\rm m}59.^{\rm s}1$	$-68^\circ04'02''$	65095
LMC155	$4^{\rm h}34^{\rm m}49.^{\rm s}4$	$-68^\circ39'32''$	71173
LMC156	$4^{\rm h}33^{\rm m}32.^{\rm s}7$	$-69^\circ15'00''$	72805
LMC157	$4^{\rm h}32^{\rm m}23.^{\rm s}8$	$-69^\circ50'26''$	44165
LMC158	$4^{\rm h}30^{\rm m}59.^{\rm s}9$	$-70^\circ26'01''$	34264
LMC159	$5^{\rm h}25^{\rm m}11.^{\rm s}4$	$-68^\circ03'58''$	234254
LMC160	$5^{\rm h}25^{\rm m}20.^{\rm s}9$	$-68^\circ39'24''$	437897
LMC161	$5^{\rm h}25^{\rm m}32.^{\rm s}5$	$-69^\circ14'59''$	787467
LMC162	$5^{\rm h}25^{\rm m}43.^{\rm s}3$	$-69^\circ50'24''$	1171172
LMC163	$5^{\rm h}25^{\rm m}52.^{\rm s}2$	$-70^\circ25'55''$	806912
LMC164	$5^{\rm h}26^{\rm m}08.^{\rm s}4$	$-71^\circ01'23''$	381352
LMC165	$5^{\rm h}26^{\rm m}20.^{\rm s}9$	$-71^\circ37'01''$	329028
LMC166	$5^{\rm h}31^{\rm m}20.^{\rm s}1$	$-68^\circ03'51''$	314715
LMC167	$5^{\rm h}31^{\rm m}39.^{\rm s}6$	$-68^\circ39'32''$	394585
LMC168	$5^{\rm h}32^{\rm m}01.^{\rm s}4$	$-69^\circ15'00''$	636559
LMC169	$5^{\rm h}32^{\rm m}22.^{\rm s}8$	$-69^\circ50'26''$	1092986
LMC170	$5^{\rm h}32^{\rm m}48.^{\rm s}1$	$-70^\circ25'53''$	878425
LMC171	$5^{\rm h}33^{\rm m}10.^{\rm s}6$	$-71^\circ01'30''$	513519
LMC172	$5^{\rm h}33^{\rm m}34.^{\rm s}4$	$-71^\circ36'54''$	423099
LMC173	$5^{\rm h}37^{\rm m}29.^{\rm s}3$	$-68^\circ03'50''$	221971
LMC174	$5^{\rm h}37^{\rm m}59.^{\rm s}8$	$-68^\circ39'26''$	340208
LMC175	$5^{\rm h}38^{\rm m}32.^{\rm s}3$	$-69^\circ15'01''$	497977
LMC176	$5^{\rm h}39^{\rm m}01.^{\rm s}6$	$-69^\circ50'30''$	576984
LMC177	$5^{\rm h}39^{\rm m}38.^{\rm s}0$	$-70^\circ25'49''$	817966
LMC178	$5^{\rm h}40^{\rm m}14.^{\rm s}1$	$-71^\circ01'27''$	471477
LMC179	$5^{\rm h}40^{\rm m}52.^{\rm s}3$	$-71^\circ36'58''$	296759
LMC180	$5^{\rm h}40^{\rm m}51.^{\rm s}5$	$-72^\circ12'28''$	258973
LMC181	$5^{\rm h}43^{\rm m}35.^{\rm s}7$	$-68^\circ03'58''$	201579
LMC182	$5^{\rm h}44^{\rm m}16.^{\rm s}0$	$-68^\circ39'32''$	311362
LMC183	$5^{\rm h}45^{\rm m}02.^{\rm s}8$	$-69^\circ14'59''$	361838
LMC184	$5^{\rm h}45^{\rm m}43.^{\rm s}2$	$-69^\circ50'33''$	486666
LMC185	$5^{\rm h}46^{\rm m}30.^{\rm s}8$	$-70^\circ25'51''$	630366
LMC186	$5^{\rm h}47^{\rm m}21.^{\rm s}2$	$-71^\circ01'24''$	376966
LMC187	$5^{\rm h}48^{\rm m}12.^{\rm s}6$	$-71^\circ36'52''$	298070
LMC188	$5^{\rm h}48^{\rm m}26.^{\rm s}6$	$-72^\circ12'27''$	152482
LMC189	$5^{\rm h}50^{\rm m}37.^{\rm s}9$	$-68^\circ39'26''$	153656
LMC190	$5^{\rm h}51^{\rm m}33.^{\rm s}2$	$-69^\circ14'55''$	200564
LMC191	$5^{\rm h}52^{\rm m}20.^{\rm s}1$	$-69^\circ50'24''$	243558
LMC192	$5^{\rm h}53^{\rm m}24.^{\rm s}1$	$-70^\circ25'51''$	228516
LMC193	$5^{\rm h}54^{\rm m}21.^{\rm s}7$	$-71^\circ01'34''$	138223
LMC194	$5^{\rm h}55^{\rm m}29.^{\rm s}7$	$-71^\circ36'59''$	77816
LMC195	$5^{\rm h}56^{\rm m}00.^{\rm s}0$	$-72^\circ12'25''$	43002
LMC196	$5^{\rm h}56^{\rm m}54.^{\rm s}7$	$-68^\circ39'29''$	116258
LMC197	$5^{\rm h}58^{\rm m}02.^{\rm s}7$	$-69^\circ15'06''$	92295
LMC198	$5^{\rm h}59^{\rm m}02.^{\rm s}5$	$-69^\circ50'35''$	71992
LMC199	$6^{\rm h}00^{\rm m}14.^{\rm s}7$	$-70^\circ26'00''$	63841
LMC200	$6^{\rm h}01^{\rm m}27.^{\rm s}5$	$-71^\circ01'36''$	58765
LMC201	$6^{\rm h}02^{\rm m}45.^{\rm s}9$	$-71^\circ37'04''$	91051
LMC202	$6^{\rm h}03^{\rm m}28.^{\rm s}3$	$-72^\circ12'34''$	79469
LMC203	$6^{\rm h}03^{\rm m}29.^{\rm s}9$	$-72^\circ48'04''$	71396
LMC204	$6^{\rm h}03^{\rm m}14.^{\rm s}6$	$-68^\circ39'25''$	108173
LMC205	$6^{\rm h}04^{\rm m}32.^{\rm s}9$	$-69^\circ15'04''$	82072
LMC206	$6^{\rm h}05^{\rm m}40.^{\rm s}3$	$-69^\circ50'27''$	78179
LMC207	$6^{\rm h}07^{\rm m}04.^{\rm s}2$	$-70^\circ25'55''$	70889
LMC208	$6^{\rm h}08^{\rm m}30.^{\rm s}4$	$-71^\circ01'27''$	87619
LMC209	$6^{\rm h}10^{\rm m}07.^{\rm s}0$	$-71^\circ37'00''$	64885
LMC210	$6^{\rm h}10^{\rm m}55.^{\rm s}7$	$-72^\circ12'37''$	70282
LMC211	$6^{\rm h}11^{\rm m}22.^{\rm s}0$	$-72^\circ48'04''$	61205
LMC212	$6^{\rm h}11^{\rm m}04.^{\rm s}0$	$-69^\circ14'50''$	81878
LMC213	$6^{\rm h}12^{\rm m}17.^{\rm s}9$	$-69^\circ50'37''$	52207
LMC214	$6^{\rm h}13^{\rm m}58.^{\rm s}2$	$-70^\circ26'08''$	60410
LMC215	$6^{\rm h}15^{\rm m}36.^{\rm s}4$	$-71^\circ01'28''$	60801

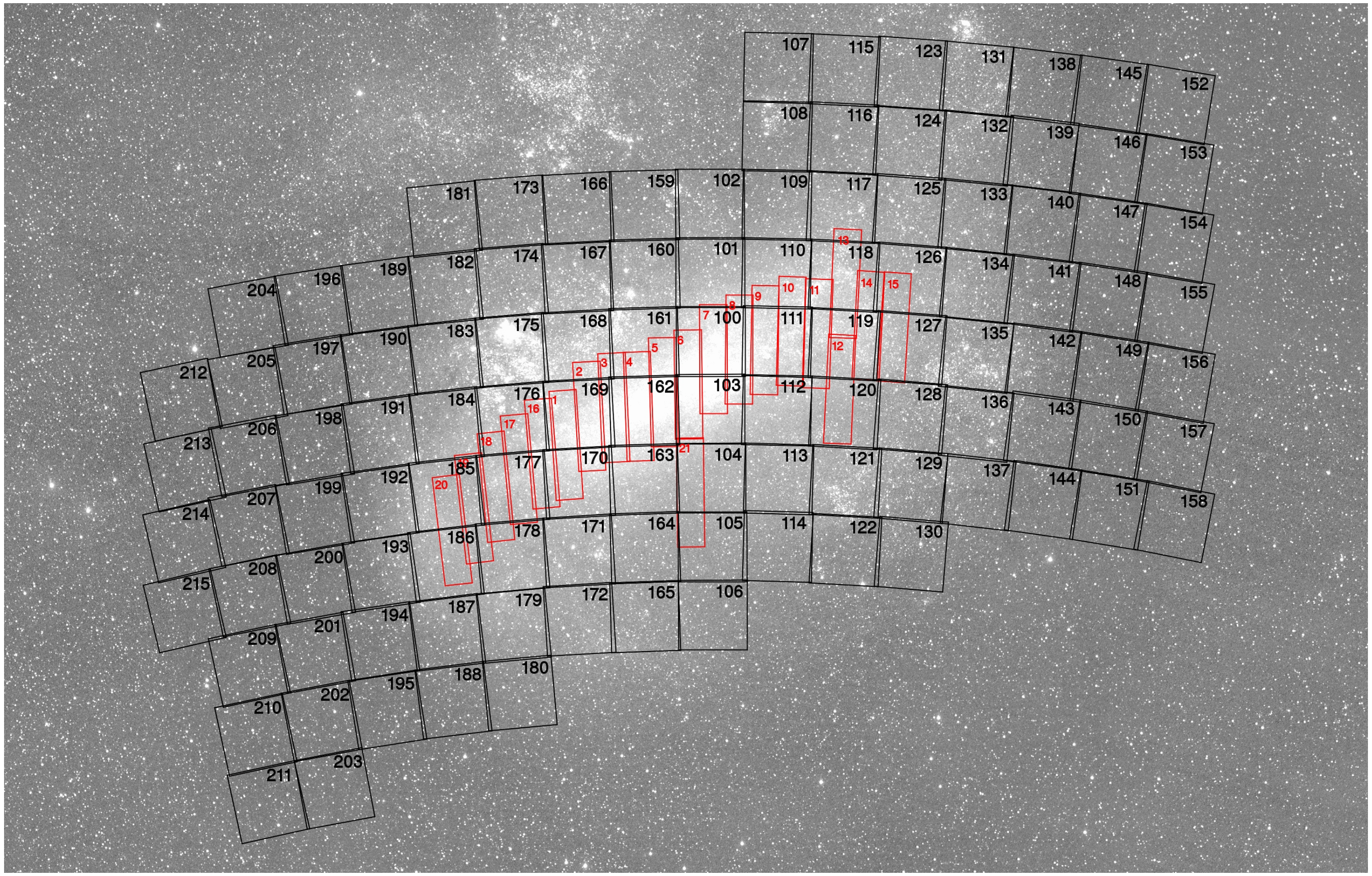

Fig. 1. OGLE-III fields in the LMC (black squares: 100–215) overplotted on the image obtained by the ASAS all sky survey. Gray strips (1–21) mark OGLE-II fields.

otometry is done also in almost real time at the telescope, photometry used in this paper comes from the final off-line re-reductions of the entire LMC dataset collected so far. Photometry is based on the Difference Image Analysis method (DIA – Alard and Lupton 1998, Woźniak 2000) and all details on the OGLE-III implementation and calibration to the standard system can be found in Udalski *et al.* (2008). Comparison with the OGLE-II photometric maps indicates that the mean difference of the magnitudes between the calibrated OGLE-III and OGLE-II photometry for about 800000 stars brighter than $I < 18$ mag and $V < 19$ mag in overlaping fields is negligible ($-0.004 \pm 0.013, -0.003 \pm 0.013$ in the I and V, respectively when calibrating directly with standard stars from Landolt's (1992) fields or $0.001 \pm 0.010, 0.000 \pm 0.007$ for final calibrations of OGLE-III photometry with OGLE-II maps) implying that OGLE-II and OGLE-III maps are photometrically fully consistent.

Astrometric transformation of the pixel grid to equatorial system was done in similar way as in the OGLE-II maps. Details can also be found in Udalski *et al.* (2008).

4. Construction of Photometric Maps

Because the OGLE-III photometric databases are constructed separately for I and V-band data, the first step of map preparation was the cross-identification of V-band counterparts to each I-band object. Due to some shifts between respective I and V-band reference images of a given subfield and larger than single detector dimensions size of the reference images to mask the gaps between chips of the OGLE-III mosaic camera, the V-band counterparts of objects located close to the border in the I-band reference image may be present in more than one field. Therefore in the first step third order transformation between pixel grids of a given I-band subfield reference image and all V-band reference images of subfields that even partially overlap were derived. Then for all I-band database objects of a given subfield their corresponding V-band counterparts in all fields were found.

The mean photometry was derived for all objects with minimum of 4 and 6 observations in the V and I-band, respectively, by averaging all observations after removing 5σ deviating points. In the case of multiple V-band cross-identifications all V-band observations formed a single dataset and then were averaged because they are independent measurements. Finally, the color term correction was applied for each object to its database average magnitude according to the transformation equations and color term coefficients presented in Udalski *et al.* (2008). After the transformation of the $V - I$ color to the standard system, I and V magnitudes were appropriately adjusted. For objects that do not have color information the average color of the LMC population $V - I = 0.7$ mag was used for color correction of respective I or V magnitude.

T a b l e 2

OGLE-III Photometric Map of the LMC100.1 subfield.

ID	RA (2000)	DEC (2000)	X	Y	V	$V-I$	I	N_V	$N_V^{\rm bad}$	σ_V	N_I	$N_I^{\rm bad}$	σ_I
1	$5^{h}19^{m}05^{s}.97$	$-69^{\circ}33'17''.4$	57.08	56.26	16.647	2.483	14.164	35	0	0.127	6	0	0.058
2	$5^{h}19^{m}08^{s}.62$	$-69^{\circ}32'15''.3$	296.00	110.54	16.331	1.922	14.409	67	−1	0.208	399	0	0.077
3	$5^{h}19^{m}08^{s}.67$	$-69^{\circ}30'56''.1$	600.20	112.84	17.715	3.062	14.652	47	0	0.157	399	0	0.065
4	$5^{h}19^{m}09^{s}.13$	$-69^{\circ}30'39''.7$	663.16	122.23	16.318	1.847	14.471	48	0	0.018	402	0	0.010
5	$5^{h}19^{m}10^{s}.04$	$-69^{\circ}29'46''.7$	866.65	141.47	14.495	0.354	14.141	48	0	0.005	402	0	0.007
6	$5^{h}19^{m}11^{s}.95$	$-69^{\circ}32'00''.9$	351.08	177.73	17.470	3.182	14.288	44	0	0.680	404	0	0.214
7	$5^{h}19^{m}13^{s}.76$	$-69^{\circ}30'00''.3$	814.39	216.32	16.530	2.092	14.438	48	0	0.029	404	0	0.015
8	$5^{h}19^{m}14^{s}.12$	$-69^{\circ}29'03''.2$	1033.50	224.43	14.141	0.188	13.953	48	0	0.004	404	0	0.006
9	$5^{h}19^{m}14^{s}.53$	$-69^{\circ}32'48''.2$	168.82	228.84	16.917	2.326	14.591	87	−1	0.072	385	0	0.033
10	$5^{h}19^{m}16^{s}.07$	$-69^{\circ}30'03''.1$	803.47	262.79	14.739	0.780	13.959	48	0	0.005	404	0	0.005
11	$5^{h}19^{m}17^{s}.31$	$-69^{\circ}31'47''.3$	402.93	285.85	15.366	1.367	13.998	48	0	0.006	404	0	0.005
12	$5^{h}19^{m}17^{s}.46$	$-69^{\circ}29'50''.9$	850.10	290.92	16.813	2.172	14.641	48	0	0.072	404	0	0.031
13	$5^{h}19^{m}19^{s}.14$	$-69^{\circ}30'12''.7$	766.32	324.45	17.416	3.007	14.408	47	0	0.286	404	0	0.189
14	$5^{h}19^{m}19^{s}.61$	$-69^{\circ}32'51''.7$	155.22	330.93	16.432	2.245	14.187	84	−1	0.048	366	0	0.021
15	$5^{h}19^{m}19^{s}.54$	$-69^{\circ}31'44''.6$	413.08	330.83	16.979	2.371	14.608	48	0	0.131	404	0	0.062
16	$5^{h}19^{m}23^{s}.42$	$-69^{\circ}33'20''.3$	44.83	407.14	16.310	9.999	99.999	40	0	0.052	0	0	9.999
17	$5^{h}19^{m}25^{s}.72$	$-69^{\circ}29'44''.3$	874.65	457.67	15.044	1.200	13.844	48	0	0.006	404	0	0.004
18	$5^{h}19^{m}27^{s}.42$	$-69^{\circ}31'18''.7$	511.94	489.95	15.476	1.214	14.262	48	0	0.008	404	0	0.005
19	$5^{h}19^{m}27^{s}.78$	$-69^{\circ}30'30''.2$	698.01	498.27	14.010	9.999	99.999	48	0	0.153	0	0	9.999
20	$5^{h}19^{m}29^{s}.18$	$-69^{\circ}30'57''.9$	591.71	525.78	13.920	−0.135	14.055	48	0	0.006	404	0	0.008
21	$5^{h}19^{m}32^{s}.47$	$-69^{\circ}30'34''.9$	679.44	592.49	15.383	9.999	99.999	48	0	0.061	0	0	9.999
22	$5^{h}19^{m}32^{s}.64$	$-69^{\circ}30'32''.9$	687.26	596.09	16.676	9.999	99.999	48	0	0.026	0	0	9.999
23	$5^{h}19^{m}33^{s}.45$	$-69^{\circ}30'18''.0$	744.46	612.71	14.765	1.573	13.192	48	0	0.008	404	0	0.006
24	$5^{h}19^{m}33^{s}.84$	$-69^{\circ}30'18''.0$	744.28	620.53	14.906	1.322	13.584	48	0	0.008	404	0	0.007
25	$5^{h}19^{m}37^{s}.93$	$-69^{\circ}31'46''.7$	402.99	700.88	15.501	2.142	13.359	48	0	0.046	404	0	0.017

Table 2 presents the first 25 entries from the map of the LMC100.1 subfield. The columns contain: (1) ID number; (2,3) equatorial coordinates J2000.0; (4,5) X,Y pixel coordinates in the *I*-band reference image; (6,7,8) photometry: *V*, $V-I$, *I*; (9,10,11) number of points for average magnitude in *V*, number of 5σ removed points in *V*, σ of magnitude for *V*-band; (12,13,14) same as (9,10,11) for the *I*-band. 9.999 or 99.999 markers mean "no data". -1 in column (10) indicates multiple *V*-band cross-identification (the average magnitude and standard deviation are calculated for merged photometry).

The full set of the OGLE-III Photometric Maps is available from the OGLE Internet archive (see below).

5. Discussion

OGLE-III Photometric Maps form a significant extension of the OGLE-II maps that covered only central regions of the LMC (*cf.* Fig. 1). The new maps include practically entire area of the LMC and can be used for many projects studying the global structure of this galaxy. Precise, well calibrated *VI* photometry and astrometry makes this dataset a unique tool for many astrophysical applications.

To show the accuracy of the OGLE-III Photometric Maps Figs. 2 and 3 present standard deviation of magnitudes as a function of magnitude in the *V* and *I*-band for two LMC fields: LMC100.1 – very dense field located in the central bar and LMC209.1 – sparsely populated field form the outer parts of this galaxy. As one can expect the accuracy of photometry depends on the stellar density and, for example, $\sigma = 0.1$ mag photometry scatter is reached for stars by about 0.3 magnitude brighter in the densest bar fields than in the uncrowded fields.

Figs. 4 and 5 show the histograms of objects in the *V* and *I*-band for the same two fields. One can notice that the completeness of the maps is high and reaches $V \approx 20.5-21$ mag and $I \approx 20-20.5$ mag. Again, as one can expected, completeness is a function of stellar crowding.

Figs. 6–9 show several color–magnitude diagrams (CMDs) constructed directly from the OGLE-III maps. They include CMD of one of the densest central fields of the LMC: LMC100.1, high extinction region near the Tarantula nebula: LMC175.6, as well as regions in the outskirts of this galaxy (LMC121.1 in the western wing and LMC186.1 in the eastern wing). Figs. 6–9 clearly illustrate the quality of data and reveal in details the characteristic features of the LMC stellar populations, as well as show how interstellar extinction affects the CMDs.

6. Data Availability

The OGLE-III Photometric Maps of the LMC are available to the astronomical community from the OGLE Internet Archive:

http://ogle.astrouw.edu.pl *ftp://ftp.astrouw.edu.pl/ogle3/maps/lmc/*

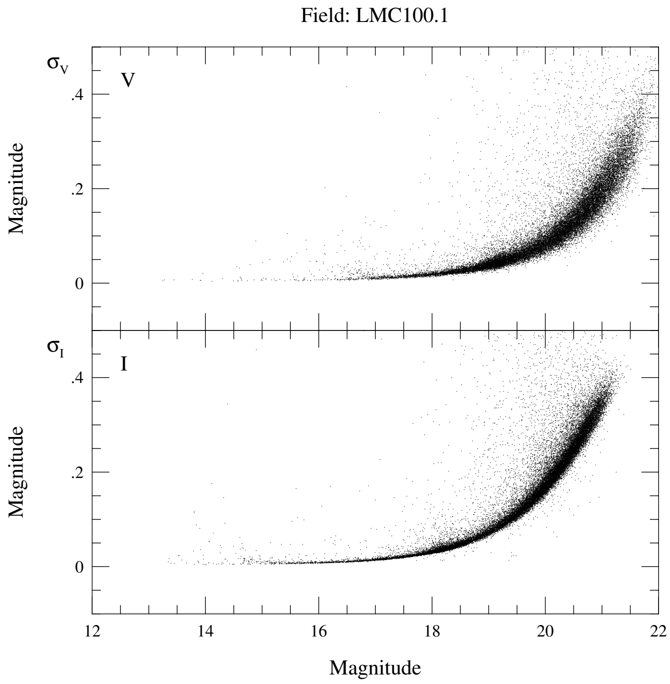

Fig. 2. Standard deviation of magnitudes as a function of magnitude for the central bar subfield LMC100.1.

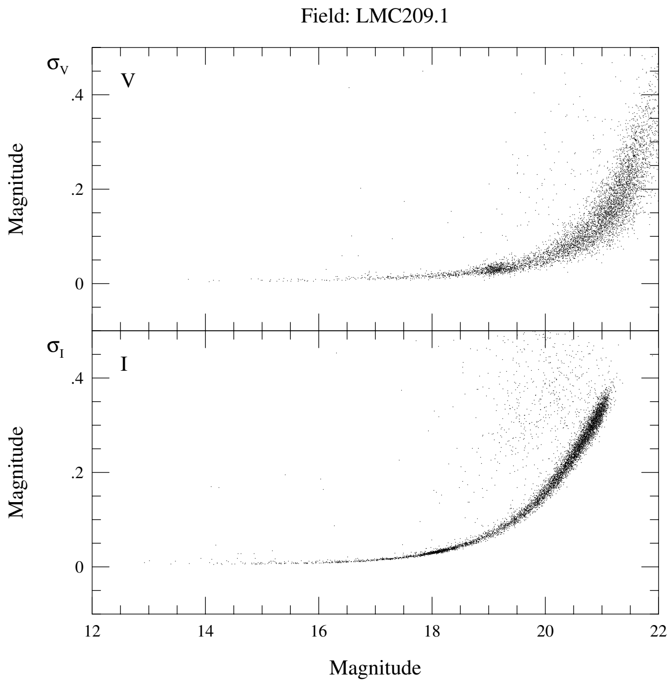

Fig. 3. Same as in Fig. 2 for the outer subfield LMC209.1

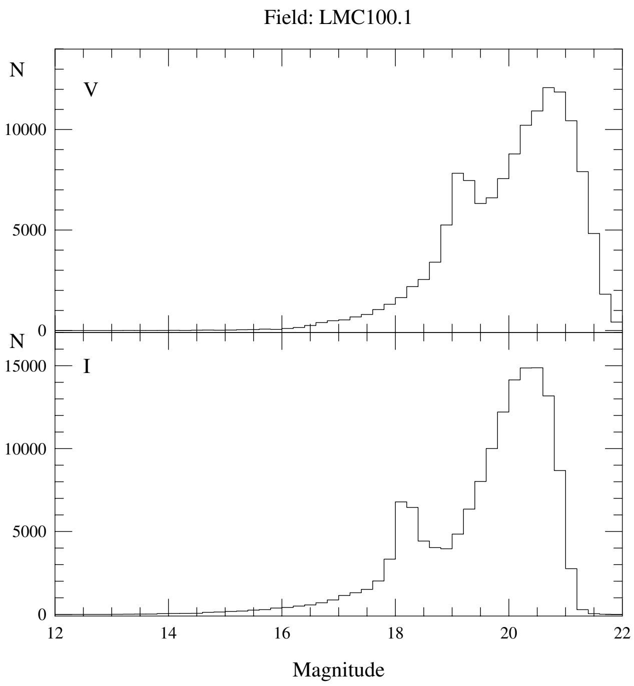

Fig. 4. Histogram of magnitudes for the central bar subfield LMC100.1.

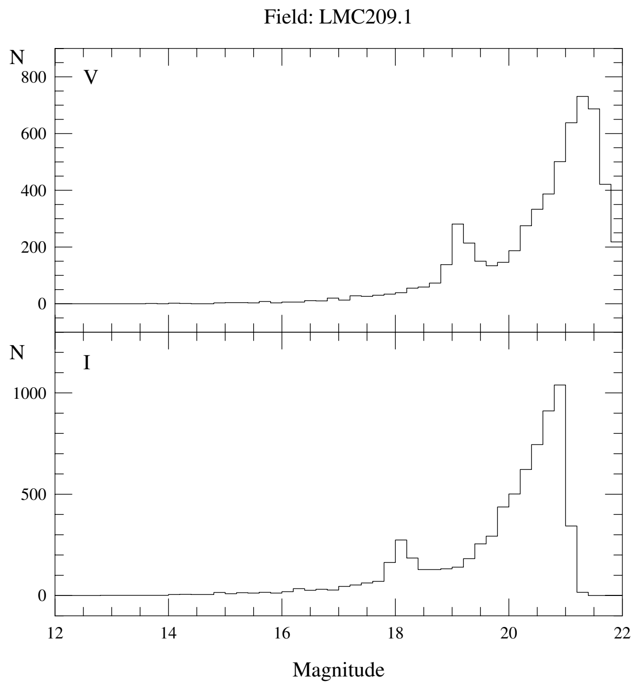

Fig. 5. Same as in Fig. 5 for the outer subfield LMC209.1.

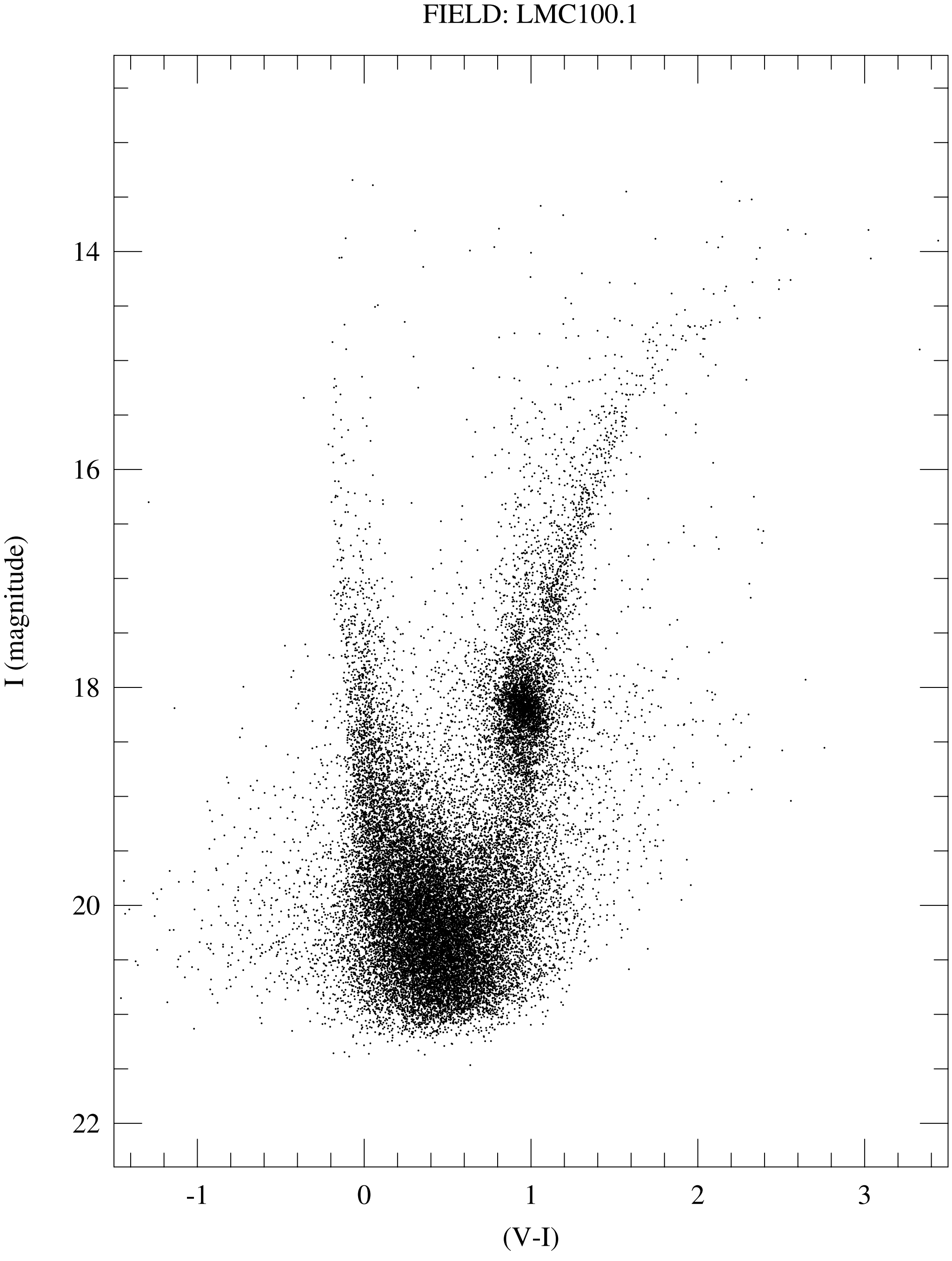

Fig. 6. Color–magnitude diagram for the central bar subfield LMC100.1.

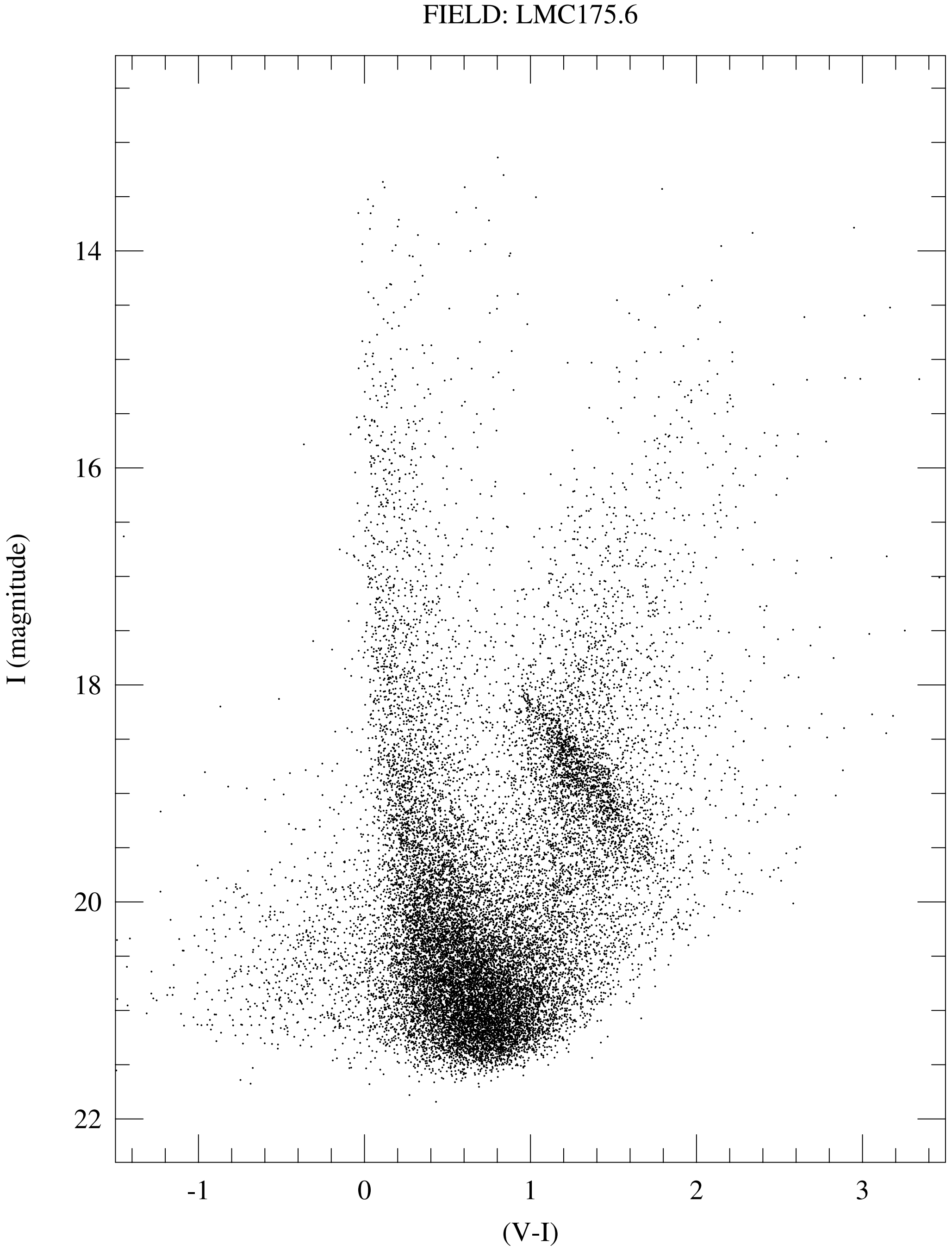

Fig. 7. Color–magnitude diagram for the variable extinction subfield LMC175.6.

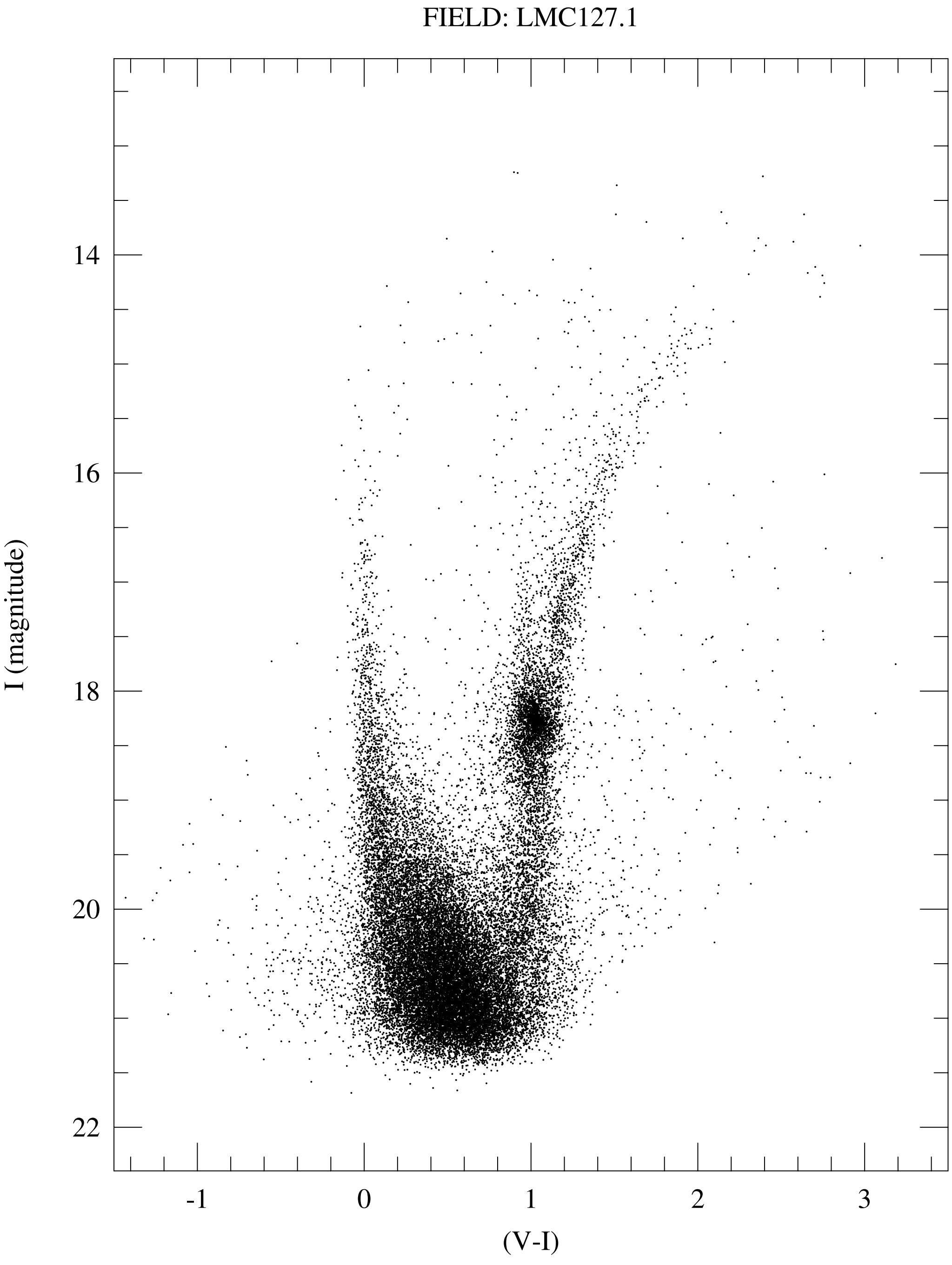

Fig. 8. Color–magnitude diagram for the western wing subfield LMC121.1

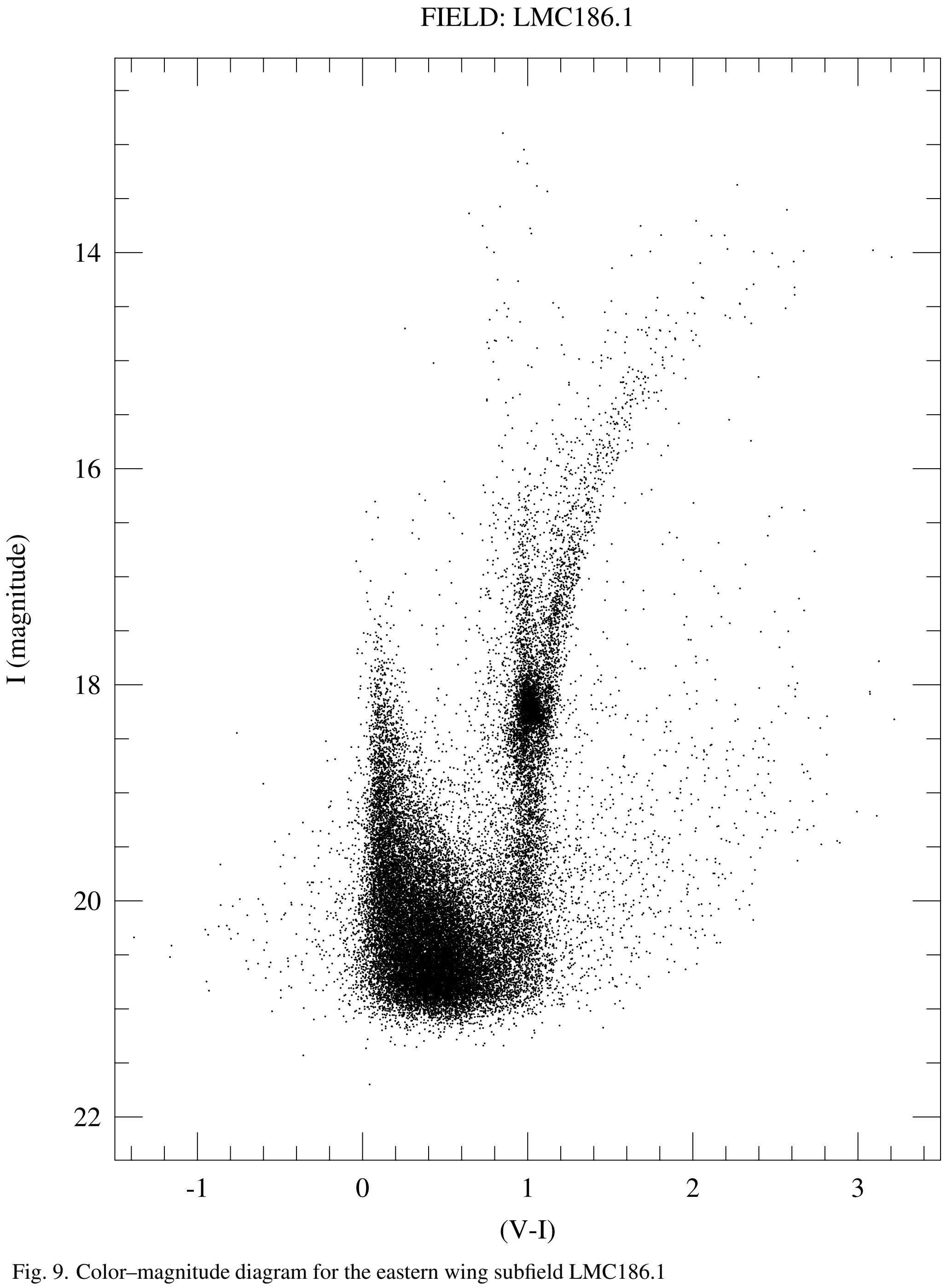

Fig. 9. Color–magnitude diagram for the eastern wing subfield LMC186.1

Beside tables with photometric data and astrometry for each of the subfields the *I*-band reference images are also included. Usage of the data is fully allowed, requiring only the proper acknowledgment to the OGLE project.

Acknowledgements. This paper was partially supported by the Polish MNiSW grant N20303032/4275 to AU and NN203293533 to IS and by the Foundation for Polish Science through the Homing Program.

REFERENCES

Alard, C., and Lupton, R. 1998, *ApJ*, **503**, 325.
Landolt, A.U. 1992, *AJ*, **104**, 372.
Pojmański, G. 1997, *Acta Astron.*, **47**, 467.
Udalski, A. 2003, *Acta Astron.*, **53**, 291.
Udalski, A., Szymański, M., Kubiak, M., Pietrzyński, G., Woźniak, P., and Żebruń, K. 1998, *Acta Astron.*, **48**, 147.
Udalski, A., Szymański, M., Kubiak, M., Pietrzyński, G., Soszyński, I., Woźniak, P., and Żebruń, K. 2000, *Acta Astron.*, **50**, 307.
Udalski, A., Szymański, M., Kubiak, M., Pietrzyński, G., Soszyński, I., Woźniak, P., Żebruń, K., Szewczyk, O., and Wyrzykowski, Ł. 2000, *Acta Astron.*, **52**, 217.
Udalski, A., Szymański, M.K., Soszyński, I., and Poleski, R. 2008, *Acta Astron.*, **58**, 69.
Woźniak, P.R. 2000, *Acta Astron.*, **50**, 421.